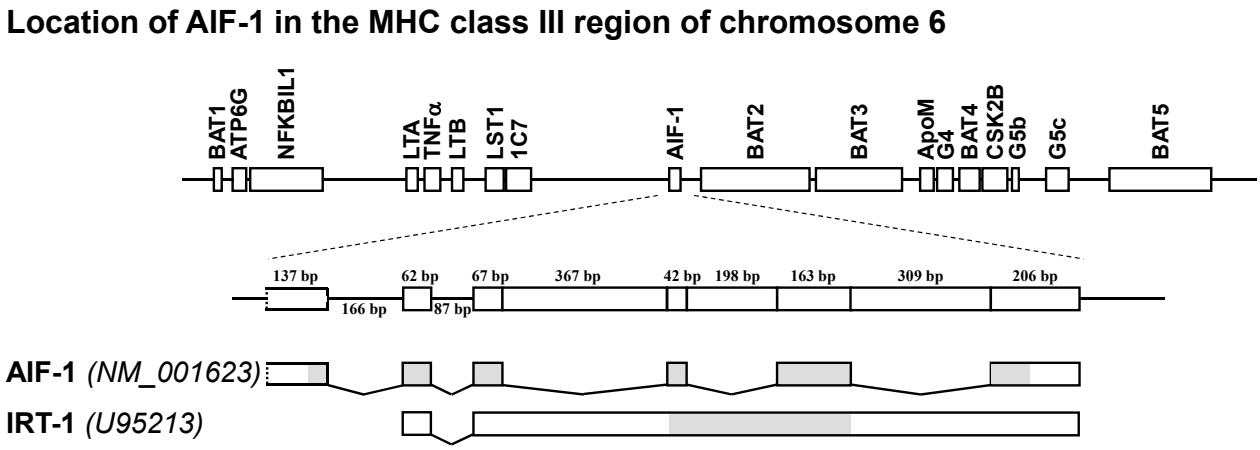

Figure S1. AIF-1 and IRT-1 are splice variants of the AIF-1 gene. Schematic representation of part of the human MHC class III region on chromosome 6, harboring the AIF-1 gene. Below is the exon/intron (boxes/lines) organization of the alternative transcripts of AIF-1 and IRT-1 (GenBank accession numbers NM_001623 and U95213, respectively). Exon/intron junctions of these transcripts conform to the consensus GT/AG rule of donor/acceptor splice site recognition. AIF-1 and IRT-1 protein coding sequences of the mRNA are shown in grey and untranslated regions (UTRs) in white.

Fig. S1

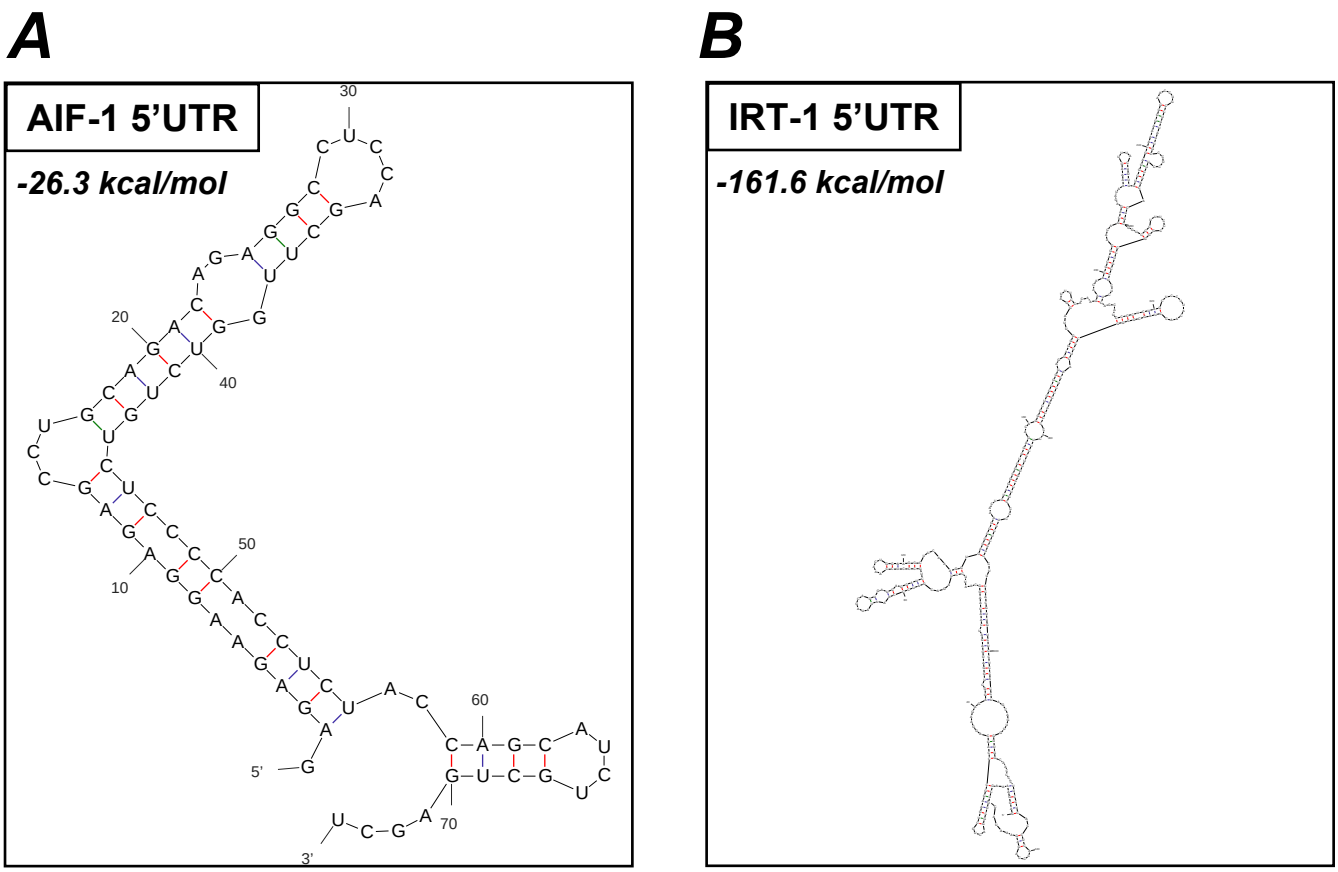

Figure S2. The secondary structure of the 5' UTRs predicted using the *mfold* version 3.2 online program is shown for AIF-1 (A) and IRT-1 (B). The 74 nt 5' UTR of AIF-1 was predicted to yield a change in free energy of -26.3 kcal/mol. For the 453 nt long 5'UTR of IRT-1, the predicted change in free energy was -161.6 kcal/mol.

Fig. S2

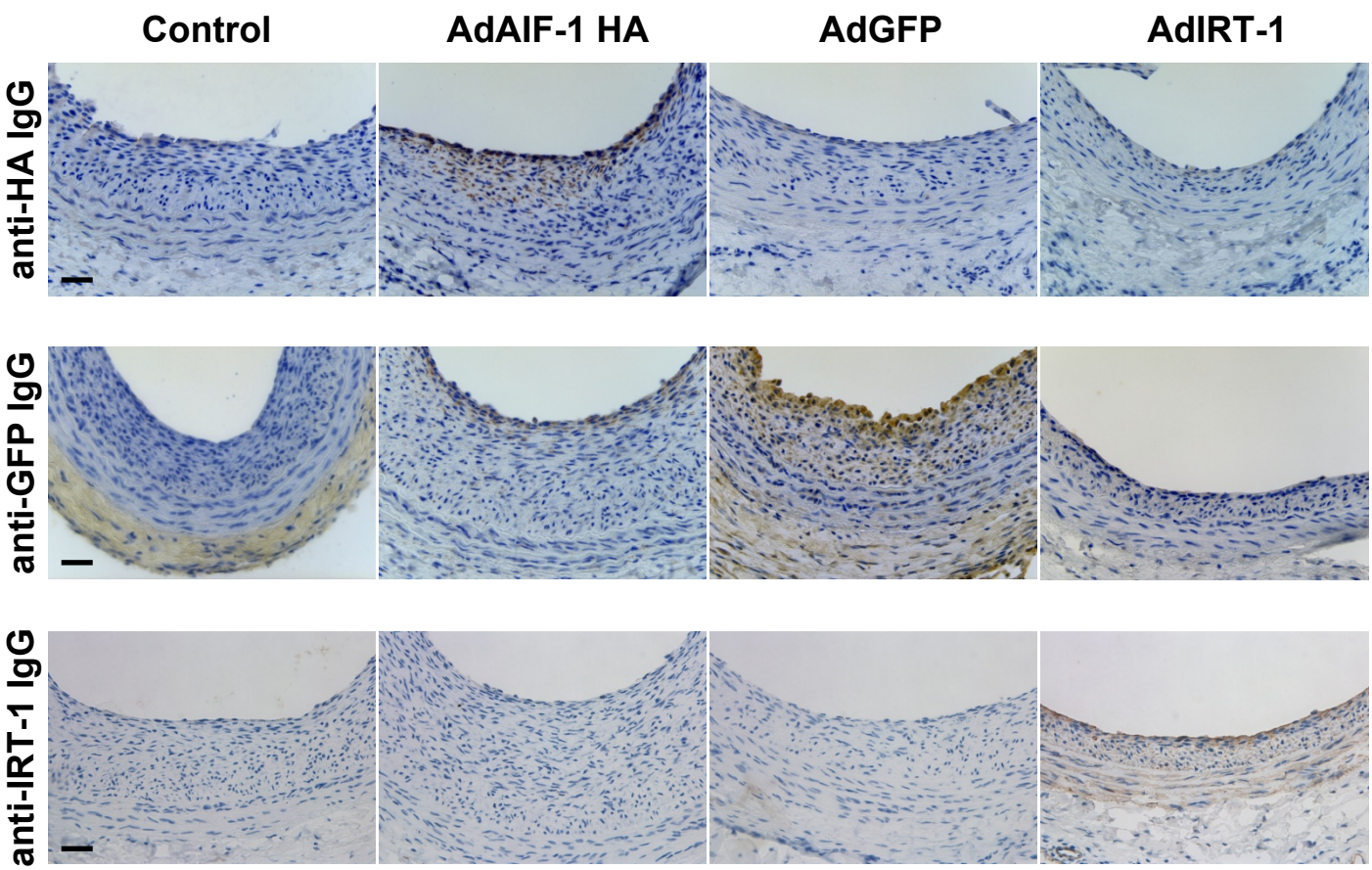

Figure S3. Adenoviral gene transfer results in protein over expression in the vascular wall. Representative sections from balloon-injured carotid arteries treated as in Figure 2A are shown. Injured arteries were infected with AdAIF-1, AdIRT-1 and AdGFP, or vehicle (PBS) and after 14 days, vessels were harvested and prepared for immunohistochemistry. Sections were stained with antibodies against either HA (for HA-tagged AIF-1, upper panels), GFP (middle panels) or IRT-1 (lower panels) and red-brown indicates positive immunoreactivity (400x magnification). All sections were counterstained with hematoxylin to visualize the nuclei. Scale bars=50 μm.

Fig. S3

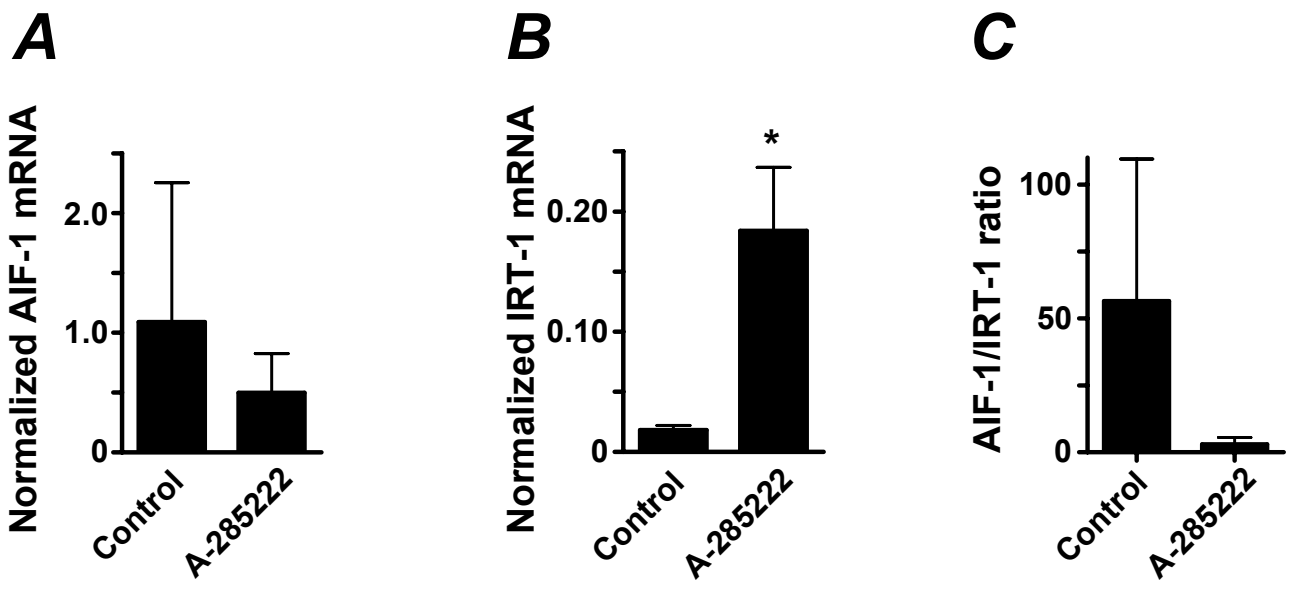

Figure S4. Inhibition of NFAT with A-285222 increases IRT-1 mRNA expression in VSMCs. Summarized data from quantitative real-time PCR showing **A.** AIF-1; **B.** IRT-1 mRNA expression and **C.** AIF-1/IRT-1 ratio in HCASMCs. The cells were cultured for 6-9 h in the presence or absence of A-285222 (1.0 μM). Expression of AIF-1 and IRT-1 was normalized to HPRT and cyclophilin A. *$p<0.05$ vs. control, n=3.

Fig. S4

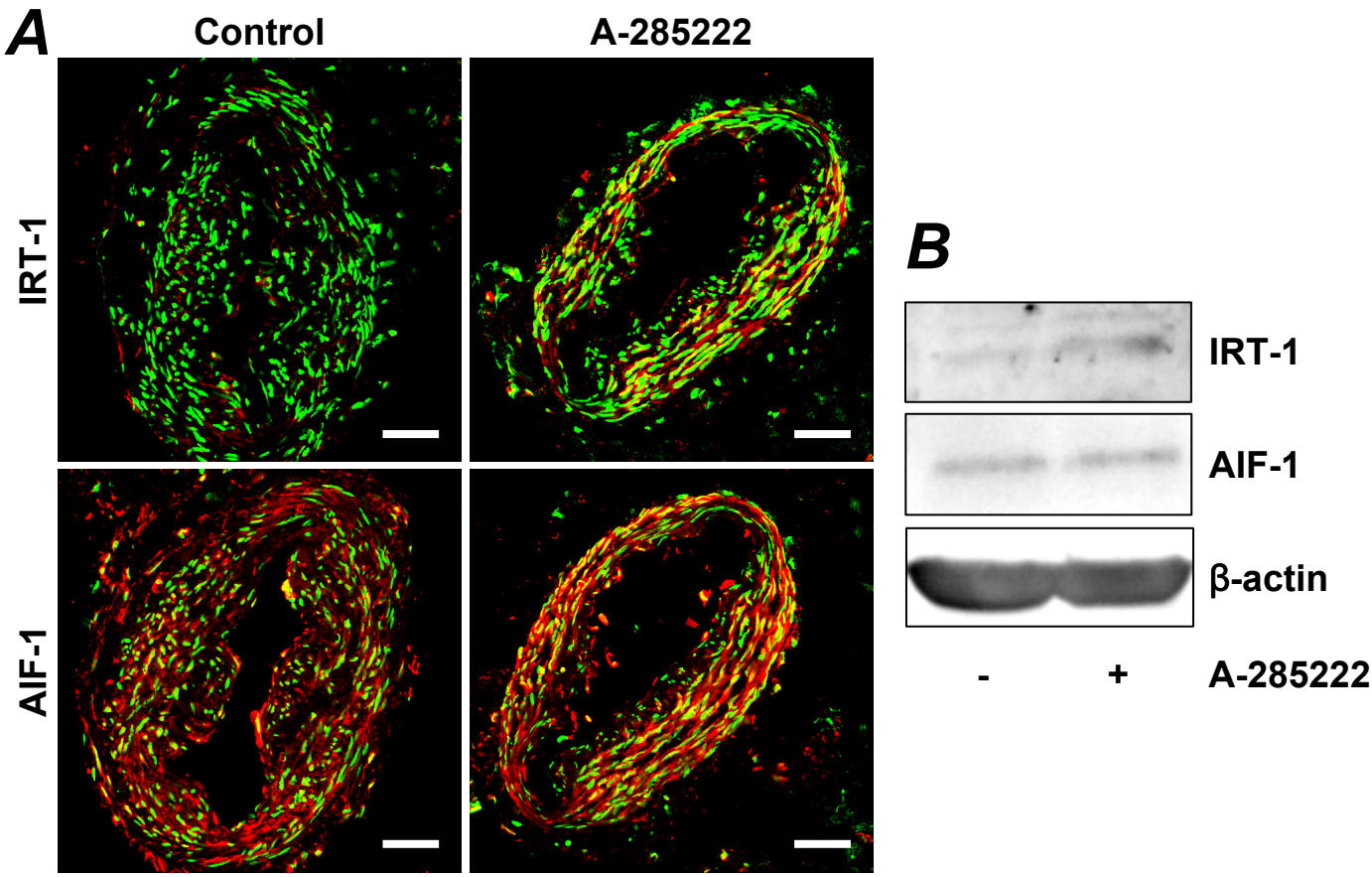

Figure S5. Inhibition of NFAT increases IRT-1 protein expression in human resistance arteries. A. Confocal images showing sections from myometrial arteries that had been cultured for 3 days in the presence or absence of the NFAT blocker A-285222 (0.1 μM). Left panels show sections from the same control artery immunostained for either IRT-1 or AIF-1 (both in red); right panels show sections from the same A-285222-treated artery. Nuclei were stained with Sytox Green. Scale bars = 50 μm. Results are representative of 2 experiments including 6 arteries for each condition. **B.** Western blot showing expression of IRT-1 (upper panel) and AIF-1 (middle panel) protein in arteries treated as in A. Expression of β-actin was used to verify equal loading.

Fig. S5

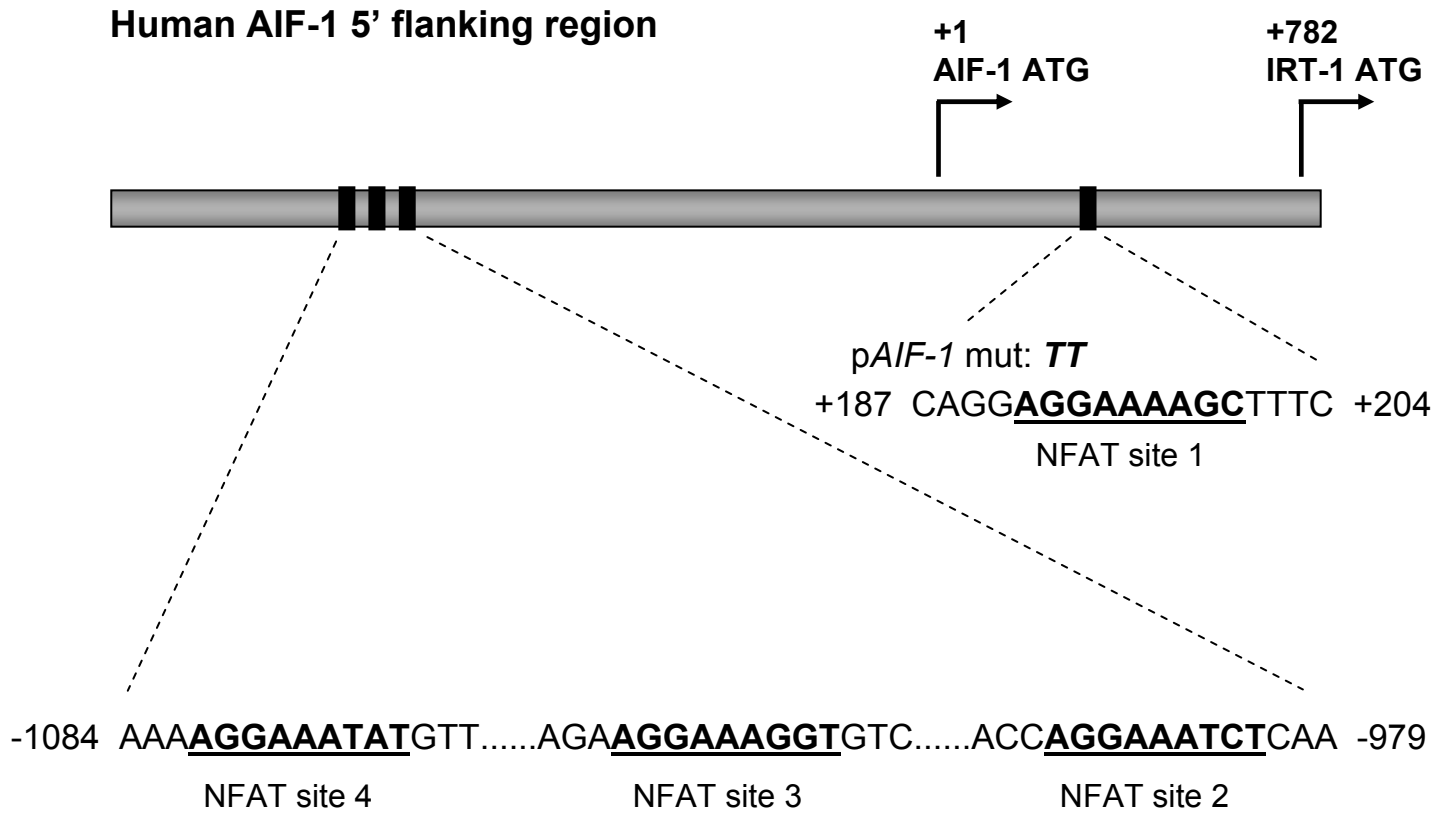

Figure S6. NFAT binding sites in the human AIF-1/IRT-1 promoter. Schematic representation of a ~2 kb region of the human genome upstream the IRT-1 protein coding region showing the location and sequences of NFAT binding sites 1-4. Numbers are relative to the AIF-1 translation start site.

Fig. S6